

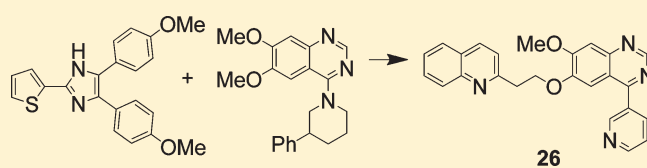
Use of Structure-Based Design to Discover a Potent, Selective, In Vivo Active Phosphodiesterase 10A Inhibitor Lead Series for the Treatment of Schizophrenia

Christopher J. Helal,* Zhijun Kang, Xinjun Hou, Jayvardhan Pandit, Thomas A. Chappie, John M. Humphrey, Eric S. Marr, Kimberly F. Fennell, Lois K. Chenard, Carol Fox, Christopher J. Schmidt, Robert D. Williams, Douglas S. Chapin, Judith Siuciak, Lorraine Lebel, Frank Menniti, Julia Cianfrogna, Kari R. Fonseca, Frederick R. Nelson, Rebecca O'Connor, Mary MacDougall, Laura McDowell, and Spiros Liras

Pfizer Worldwide Research and Development, Eastern Point Road, Groton, Connecticut 06340, United States

S Supporting Information

ABSTRACT: Utilizing structure-based virtual library design and scoring, a novel chimeric series of phosphodiesterase 10A (PDE10A) inhibitors was discovered by synergizing binding site interactions and ADME properties of two chemotypes. Virtual libraries were docked and scored for potential binding ability, followed by visual inspection to prioritize analogs for parallel and directed synthesis. The process yielded highly potent and selective compounds such as **16**. New X-ray cocrystal structures enabled rational design of substituents that resulted in the successful optimization of physical properties to produce in vivo activity and to modulate microsomal clearance and permeability.



INTRODUCTION

Phosphodiesterases (PDEs) constitute a family of enzymes that hydrolyze the ubiquitous intracellular messenger molecules cyclic guanosine monophosphate (cGMP) and cyclic adenosine monophosphate (cAMP), a process that regulates the activity of these molecules which have a role in essentially all physiological functions.¹ The PDEs are divided into 11 families, with members of a given family demonstrating similar substrate specificity as well as inhibition by pharmacological tools. The central role played by PDEs in regulating physiological function has resulted in extensive efforts to identify inhibitors specific for a PDE family. This effort has elucidated the role of these enzymes in various biological processes to identify therapeutic opportunities among this class of enzymes. Central to the generation of specific inhibitors is the ability to determine the three-dimensional structure of PDEs via X-ray crystallography that can enable a guided approach to inhibitor design and optimization.^{2,3}

Phosphodiesterase 10A (PDE10A), a phosphodiesterase that hydrolyzes both cGMP and cAMP, is expressed highly in the medium spiny neurons of the striatum.⁴ Recent work has shown that blockade of PDE10A with selective inhibitors increases striatal cGMP and phosphorylated CREB, a downstream marker of cAMP production.^{3,5} In conditioned avoidance responding (CAR), an animal model predictive of drug antipsychotic activity, PDE10A inhibitors produce a dose-dependent inhibition, an effect which is absent in PDE10A knockout mice, thus supporting this activity being specifically due to PDE10A inhibition.⁵

With an interest in being able to examine the effect of a PDE10A inhibitor in a clinical setting, we sought to bring forward

a number of structurally diverse chemical series that would increase the chances of finding a compound with the appropriate in vivo potency, pharmacokinetic properties, and safety. In particular, we sought a compound with PDE10A $IC_{50} < 10$ nM and low to moderate intrinsic human liver microsomal clearance (HLM Cl_{int}) (< 48 mL/min/kg). To achieve good blood-brain barrier permeability, we also pursued PDE10A inhibitors with no evidence of P-glycoprotein (Pgp)-mediated efflux in an in vitro transporter assay (MDR BA/AB < 2).⁶

RESULTS AND DISCUSSION

The approach that our lab utilized started with the examination of X-ray cocrystal structures of a variety of PDE10A inhibitors from high through-put screening and initial hit-to-lead efforts, their in vitro PDE selectivity profiles, and comparison of the catalytic sites of other PDE X-ray structures to interpret the observed selectivity. Two series of PDE10A inhibitors of particular interest, quinazolines (**1**)^{3a} and triarylimidazoles (**2**),^{5b} are shown in Figure 1.

As reported previously, quinazoline **1** yielded PDE10A IC_{50} = 45 nM, but had activity at both PDE3A and PDE3B (IC_{50} = 3790 nM and 636 nM, respectively).^{3a} PDE3A/B inhibition has known effects on cardiovascular function and was thus an activity to be avoided.⁷ Examination of the X-ray crystal structure of **1** in the cyclic nucleotide binding site reveals a number of interactions that may be important for the high potency (Figure 2): 1) the

Received: February 9, 2011

Published: June 08, 2011

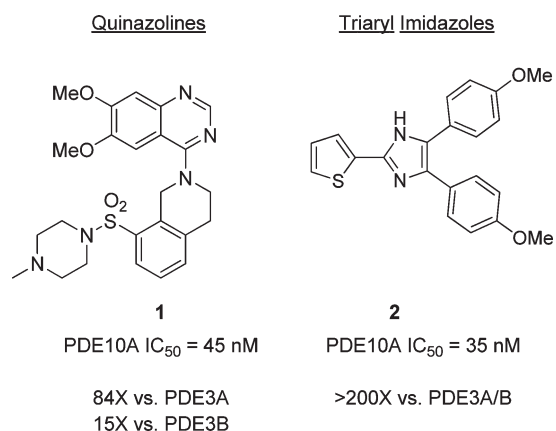


Figure 1. Representative PDE10A inhibitors **1** and **2**.

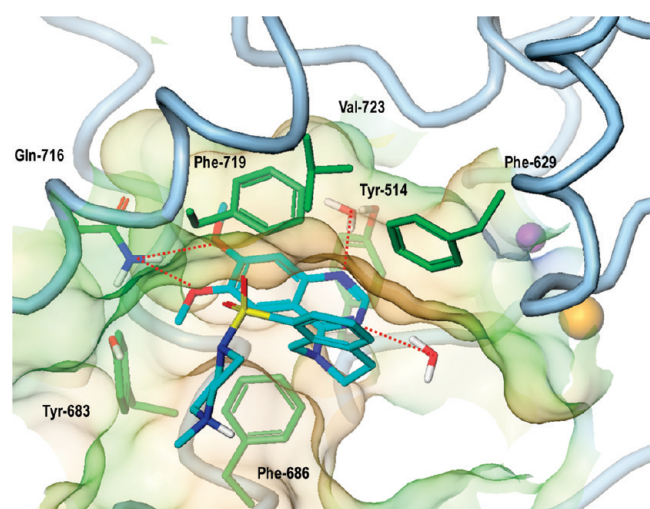


Figure 2. X-ray crystal structure of quinazoline **1** (cyan, PDB ID 2O8H) bound to PDE10A cyclic nucleotide binding site. Note: All PDE10 crystal structures described in this manuscript were obtained using a construct derived from rat PDE10 enzyme.^{3a} However, the residue numbering in this paper follows the human sequence, so as to be consistent with the other literature on this subject. Rat and human sequences are >90% identical in the catalytic domain, and the numbering of the human residues is simply (–10) from the corresponding rat residues, for example, Gln716(human) corresponds to Gln726(rat).

6,7-dimethoxy groups form a bidentate interaction with the N–H of Gln-716, a conserved amino acid residue in all PDEs that is central to the binding of endogenous cyclic nucleotides; 2) the quinazoline ring sits within a hydrophobic clamp formed by Phe-719 on the top and Phe-686 on the bottom; 3) the phenyl group of the tetrahydroisoquinoline projects out of the hydrophobic pocket and interacts with the hydrophobic wall formed by Phe-719, Val-723, and Phe-629; 4) N-1 of the quinazoline interacts with the OH of Tyr-514 via a bridging water molecule; N-3 accepts a hydrogen bond from a water that interacts with the hydration sphere of the catalytic zinc and magnesium cations.⁸ It should be noted that the piperazine sits outside of the catalytic site, presumably exposed to solvent.

In comparison, triarylimidazole **2** had PDE10A IC₅₀ = 35 nM and showed weak activity against PDE3 (PDE3A = 11% inhibition @ 1 μM; PDE3B = 18% inhibition @ 10 μM).^{3b,5} Examination of

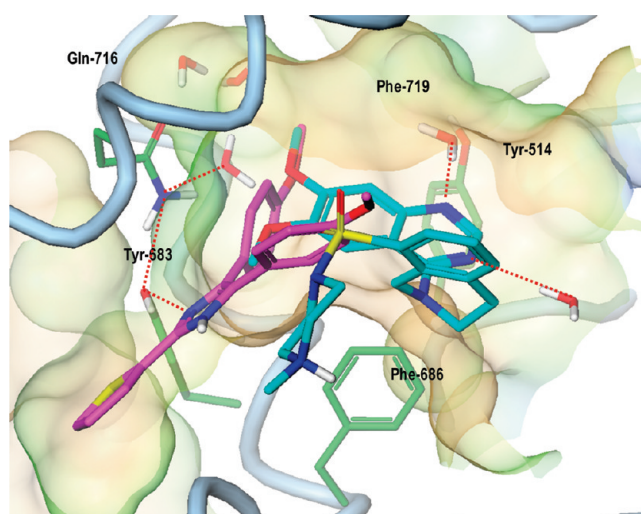


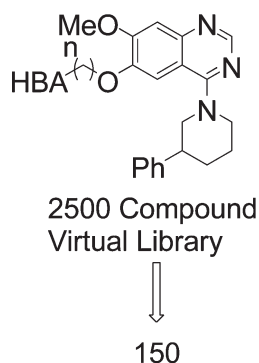
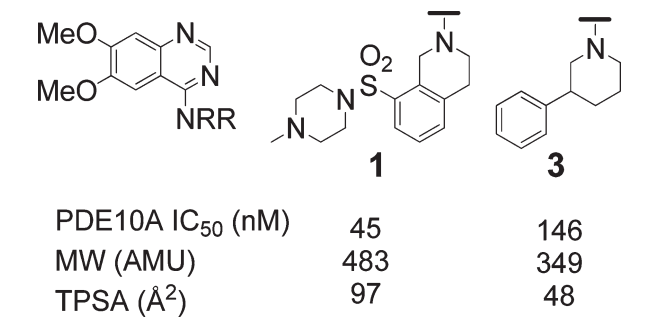
Figure 3. X-ray structure of triaryl imidazole **2** (magenta, PDB ID 3HQW) and quinazoline **1** (cyan) bound to the PDE10A cyclic nucleotide binding site.

its cocrystal structure with the PDE10A catalytic domain revealed a possible basis for this selectivity, as it showed a binding interaction that is markedly different, not just from PDE10A inhibitors, but from other PDE inhibitors in general (Figure 3). Most importantly, the thiophene occupied a lipophilic pocket near the entrance of the hydrophobic cleft that defines the substrate binding site all PDEs. A comparison of the known crystal structures and a profiling of all PDEs binding sites sequence similarity show that this pocket is unique to PDE10A among all 21 PDEs in the family and thus may explain the high selectivity demonstrated by this series.^{3b} Additionally, the imidazole accepts a hydrogen bond at the top of the pocket from the OH of Tyr-683 which accepts a hydrogen bond from the carboxamide amine of the conserved Gln-716 side chain. The other amide NH of the Gln-716 side chain forms a hydrogen bond with a buried water molecule. One 4-methoxyphenyl interacts with the Gln-716 amide side chain through van der Waals stacking contact. The second 4-methoxyphenyl makes a face-edge π interaction with Phe-719.

Considering the difference in PDE3A/B selectivity profiles of quinazoline **1** and triaryl imidazole **2**, we hypothesized that chemotypes like **1** could be made highly selective by accessing the same “selectivity pocket” that the thienylimidazole portion of **2** occupied. In particular, we sought to form an H-bond with Tyr-693 and to fill the adjacent lipophilic pocket. Based upon the overlapping X-ray crystal structures of **1** and **2**, variation of the 6-methoxy group of **1** appeared to allow access to the selectivity pocket. Also, considering the necessary orthogonal arrangement between the quinazoline and the desired group in the selectivity pocket, we reasoned that alkyl linkers would provide the optimal flexibility and thus focused efforts on these.

An additional concern in the design process was the overall physical properties of subsequent compounds that would increase in molecular weight (MW) and potentially topological polar surface area (TPSA), thus resulting in limited brain penetration. Considering that **1** had MW = 483 and TPSA = 97 Å², suggested that 6-methoxy derivatives could easily have MW >500 and TPSA >100 Å².⁹ Thus, an alternative amine to the sulfonamide tetrahydroisoquinoline (STHIQ) in **1** was sought

Scheme 1. Comparison of Properties of 1 and 3

**Selection Criteria**

- 1) Docked and scored
- 2) Visual inspection
- 3) Filtered by TPSA and MW

Figure 4. Processes to generate a virtual library targeted to the PDE10A selectivity pocket.

with similar potency but reduced MW and TPSA. As mentioned previously,^{3a} a chemical library approach to vary the amine in **1** was carried out and one of the amines that was found to afford reasonable potency with significantly lower MW and TPSA than the STHIQ was the 3-phenylpiperidine in compound **3** (Scheme 1).¹⁰ Based upon the modeled binding of **3** in the PDE10A X-ray structure, similar interactions were made as **1** with an improved ability of the 3-phenylpiperidine to form an edge-face π interaction with Phe-719. It was this amine that was thus used as part of the template for initial optimization work.

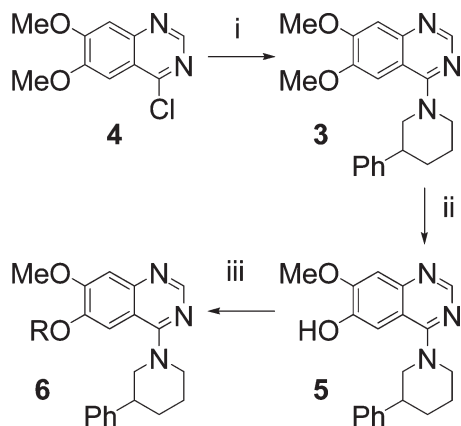
To evaluate the optimal linker length and the preferred group to fill the selectivity pocket, we built a virtual library of 2500 compounds derived from the *in silico* coupling of all available alcohols and alkyl halides available in our in-house compound file with the quinazoline 6-hydroxy group, with a particular interest in those compounds containing hydrogen-bond acceptors (HBA) that could interact with Tyr-683 (Figure 4). We docked this virtual library into the PDE10A cocrystal structure of **1**, with the quinazoline core constrained with a harmonic force to a position as in the X-ray structure of **1**.¹¹ Each molecule was docked 50 times with the piece-wise linear potential¹¹ and rescored with an in-house scoring function.¹² The best scored conformation was kept for each compound. The high scoring compounds were prioritized by the rescoring energy and visually examined, regardless of the physicochemical properties of the

Table 1. 6-Alkoxy SAR

	R	PDE10A IC ₅₀ (nM)	PDE3A IC ₅₀ (nM)
3	Me	146	8.5
7	n-Pr	1040	98
8		>3200	
9		>3200	
10		>3200	
11		>3200	
12		1665	
13		247	32% inhib @ 1 μ M
14		2338	
15		>3200	

compounds, to allow for identification of desirable binding motifs. This exercise suggested that 2-carbon linkers attached to various H-bond accepting groups would allow for optimal access to the selectivity pocket along with H-bond interactions with Tyr-683. All enumerated compounds were next filtered by calculated properties favoring brain penetration (topological polar surface area <120 Å² and molecular weight <500). Based upon this analysis, we chose to synthesize some of the top ranking compounds in a parallel format. Concomitantly, we also picked a set of compounds for directed synthesis to test our hypothesis of selectivity pocket interactions via a systematic variation of linker length and hydrogen bond acceptor positioning (Table 1).

The synthetic route to access 6-alkoxy derivatives is detailed in Scheme 2. Coupling of 3-phenylpiperidine with 4-chloro-6,7-dimethoxyquinazoline **4** gave the 4-aminoquinazoline product **3** which was then selectively demethylated using methanesulfonic acid/methionine to afford **5**. The coupling of **5** with alkyl halides to afford **6** proceeded smoothly in DMSO with cesium carbonate as base. The Mitsunobu coupling of **5** with alcohols was found to proceed efficiently only under conditions where a mixture of

Scheme 2^a

^a Reaction conditions: (i) 3-phenylpiperidine, isopropanol, diisopropylethylamine, 90 °C, 75%; (ii) methanesulfonic acid, methionine, 120–145 °C, 52%; (iii) DBAD/PPh₃, ROH or Cs₂CO₃, DMSO, RX; 30–80%.

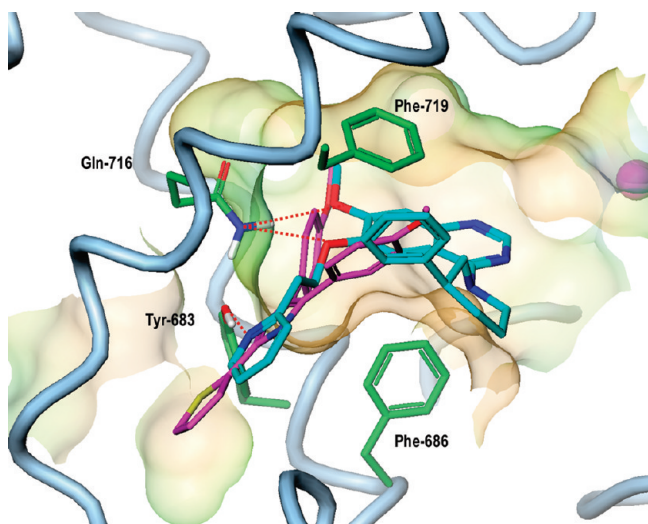


Figure 5. X-ray cocrystal structure of pyridyl ethyl analog **13** (cyan, PDB ID 3QPO) in comparison with triarylimidazole **2** (magenta).

azodicarboxylate/triphenylphosphine was first treated with the desired alcohol for 10 min followed by addition of **5**.¹³

Efforts at directed analog synthesis (Table 1) showed that increasing the 6-methoxy (**3**) to 6-*n*-propoxy (**7**) gave >10× reduction in activity without any PDE3A selectivity gain. A one carbon linker attached to the 2, 3, or 4-position of a pyridine or quinoline (**8–11**) provided further reductions in PDE10A potency. When examining analogs with a 2-carbon linker, predicted to be the optimal length from the *in silico* docking exercise, the phenyl derivative afforded little activity (**12**). The 2-pyridyl analog **13**, however, demonstrated PDE10A IC₅₀ = 247 nM as a racemate. Additionally, selectivity over PDE3A was now >5-fold as compared to being <0.1 in compounds **3** and **7**. The X-ray crystal structure of **13** bound to PDE10A confirmed the binding of the pyridyl N to Tyr-683 (Figure 5), very similar to what was modeled, and thus validated the strategy of accessing the selectivity pocket from the 6-alkoxy substituent. The 3- and 4-pyridyl analogs, **14** and **15**, showed poor PDE10A inhibition, consistent

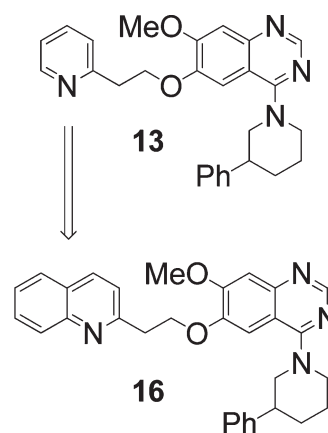
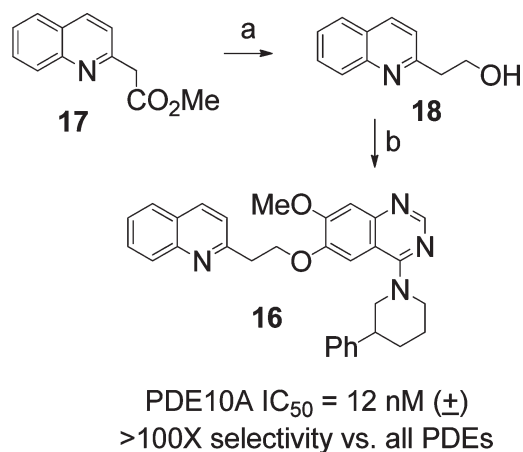


Figure 6. Proposed target **16** to improve potency and selectivity.

Scheme 3^a

^a Reaction conditions: (a) LAH, Et₂O, −78 to 0 °C, 53%; (b) di-*tert*-butyl azodicarboxylate, triphenylphosphine, **5**, THF, r.t., 30%.

with the requirement of appropriate alignment of the HBA to interact with Tyr-683.

A closer examination of the cocrystal structure of **13** suggested fusing an aryl ring onto the 2-pyridyl ring to afford quinoline **16**, which would allow for overlap of the thienyl group in **2**, would completely fill the selectivity pocket, and could provide additional potency and selectivity gain (Figure 6).

The synthesis of **16** started with reduction of ester **17** to alcohol **18** with lithium aluminum hydride in diethyl ether from −78 °C with gradual warming to 0 °C (Scheme 3). It should be noted that the use of THF as solvent or higher temperatures led to considerable quinoline reduction. Coupling of **5** with **18** under the Mitsunobu conditions described above yielded the target compound **16**, which afforded PDE10A IC₅₀ = 12 nM as a racemate.¹⁴

An X-ray cocrystal structure of **16** bound to PDE10A confirmed that the quinoline filled the selectivity pocket in a manner similar the thienylimidazole in **2** (Figure 7). This compound proved to be ≥100x selective vs all other PDEs (see Supporting Information for PDE selectivity data).

The results of parallel chemistry efforts to produce a wide range of 6-alkoxy SAR, which used the direct alkylation and Mitsunobu conditions described above, generated results that built on the result of quinoline **16**. Benzimidazole **19**, with a three-carbon

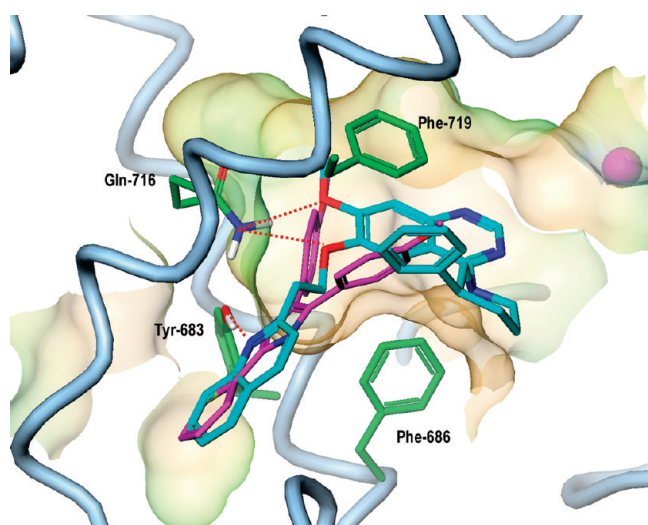


Figure 7. Overlap of quinolyethyl analog **16** (cyan, PDB ID 3QPP) with thienylimidazole **2** (magenta).

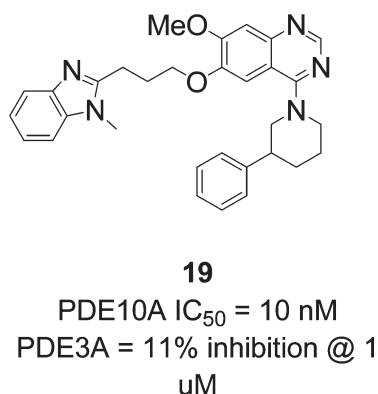


Figure 8. Benzimidazole analog from parallel chemistry efforts.

linker, was potent (PDE10A IC₅₀ = 10 nM) and showed high selectivity versus PDE3A (Figure 8).

Compounds such as **16** and **19** are highly potent and selective PDE10A inhibitors, but their ligand efficiency (LE), a measure of potency per atom,¹⁵ is reduced as compared to **3**. The increases in molecular weight and lipophilicity (cLogD) result in higher HLM Cl_{int} and significant *in vitro* Pgp efflux (Table 2).

We hypothesized that the quinoline interaction in the selectivity pocket was the major potency and selectivity “anchor” for **16**, possibly rendering the phenylpiperidine superfluous, and thus targeted truncated analogs with more desirable physicochemical properties to test this hypothesis.

We first prepared **20**, which showed a loss in potency but a significant improvement in LE (Figure 9). This result supported the hypothesis that the phenylpiperidine was not providing optimal binding efficiency in **16**, and compound **21** became the next target.

Hydrogenolysis of commercially available 2,4-dichloro-6,7-dimethoxyquinazoline gave **22** (Scheme 4). Selective acidic demethylation resulted in 7-hydroxy-6-methoxyquinazoline **23**, as opposed to the desired 6-hydroxy-7-methoxyquinazoline. This unexpected switch in regiochemistry did not allow for access to the targeted **21**. This alternative regioisomer was carried forward

Table 2. Comparison of Physicochemical and ADME Properties of **3** and **16**

PDE10A IC ₅₀	146 (±)	12 (±)
PDE3A Selec	<1×	>100×
LE	0.37	0.29
MW	349	490
cLogD	1.5	3.2
HLM Cl _{int} (mL/min/kg)	13	>19
MDR BA/AB	0.7	>10

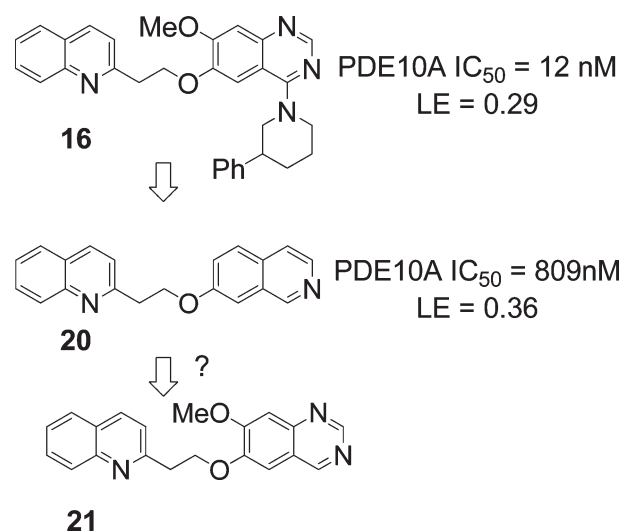
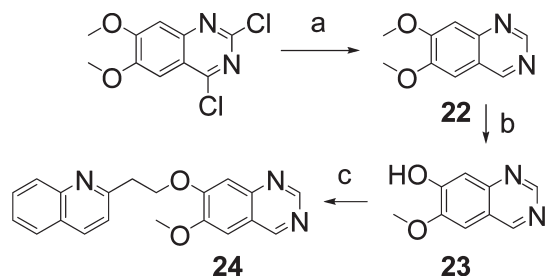


Figure 9. Improvements in LE suggest new SAR directions.

into a Mitsunobu coupling with 2-quinolyloethanol **18** and afforded **24**, which has the quinazoline nitrogens in different positions than previous quinazoline analogs. Compound **24** showed excellent potency, selectivity, ligand efficiency, low HLM Cl_{int}, no Pgp efflux, and moderate permeability. The crystal structure of **24** bound to PDE10A showed that the quinoline group interaction in the selectivity pocket was completely identical to that seen in the structure of **16** (Figure 10), confirming the role of this group as a binding ‘anchor’. It should be pointed out that the water molecules that interact with the quinazoline nitrogens in **1** were not observed in the X-ray crystal structure of **24**. This observation suggests that these bridging water interactions may be less critical when the selectivity pocket is efficiently occupied.

No activity was observed when **24** was tested for its ability to increase striatal cGMP in mouse at 5.6 mg/kg, sc. It was presumed that the moderate *in vitro* permeability could be translating into less than optimal *in vivo* brain penetration. Additionally, the necessary exposure may have been limited by high rodent specific clearance (rat microsomal Cl_{int} = 183 mL/min/kg).

Scheme 4^a

PDE10A IC₅₀ = 17 nM
 LE = 0.42
 PDE3A = 51% inhib @ 1 μM
 HLM Cl_{int} <7 ml/min/kg
 MDR BA/AB = 0.9
 MDR AB, P_{app} = 3 × 10⁻⁶ cm/sec

^a Reaction conditions: (a) Pd/C, TEA, MeOH, H₂ (40 psi), 65%; (b) L-methionine, MeSO₃H, 120–145 °C, 57%; (c) di-*tert*-butylazodicarboxylate, triphenylphosphine, **18**, THF, 38%.

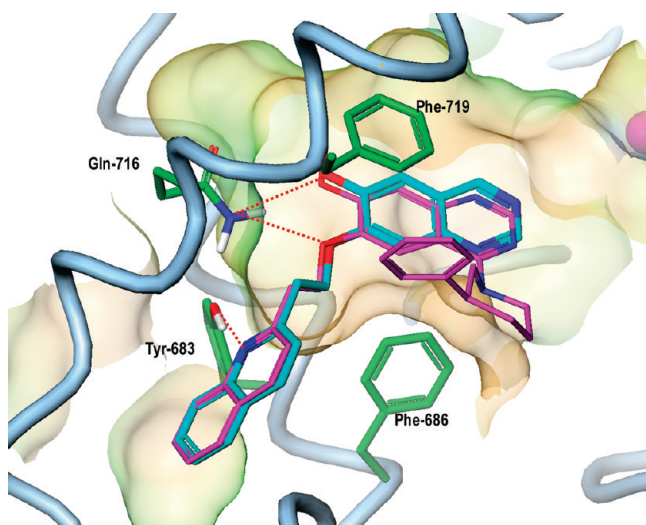
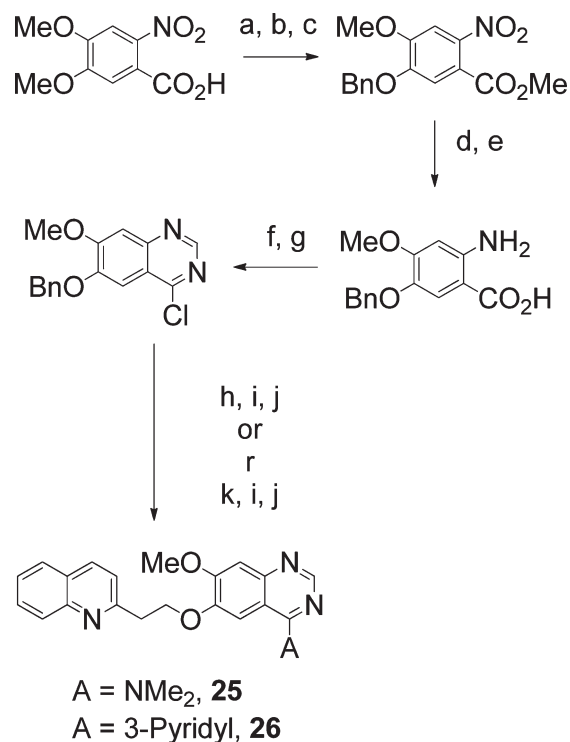


Figure 10. Overlap of **24** (cyan, PDB ID 3QPJ) and **16** (magenta).

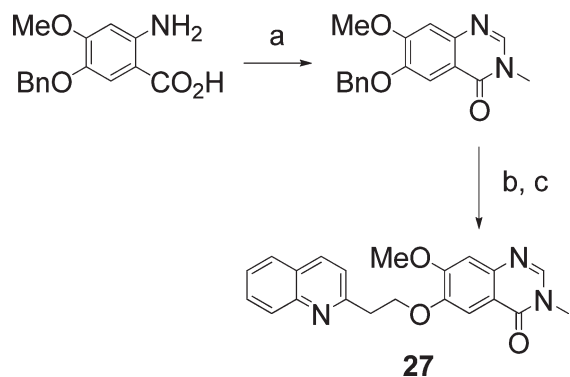
We sought to address the challenge of balancing permeability and clearance by variations on the quinazoline core. In particular, based upon the X-ray crystal structure, and the knowledge that 3-phenylpiperidine was tolerated as in **16**, structural modifications at the quinazoline 4-position were pursued (Schemes 5 and 6).

Three series of analogs were made. A comparison of representative compounds from the amino (**25**) and aryl (**26**) class, as well as quinazolinone (**27**), is shown in Table 3.

The dimethylamino quinazoline **25** and the quinazolinone **27** had similar profiles with PDE10A IC₅₀ = 14 nM and 12 nM, respectively, high permeability with no Pgp efflux, and high HLM, Cl_{int}. The 3-pyridyl quinazoline **26** afforded PDE10A IC₅₀ = 5 nM, low human microsomal clearance, no Pgp efflux, with low permeability. All compounds showed the ability to increase brain cGMP in mouse in vivo to differing degrees (See Supporting Information). On the basis of the low human

Scheme 5^a

^a Reaction conditions: (a) NaOH, H₂O, 100 °C, 99%; (b) H₂SO₄, MeOH, reflux, 96%; (c) BnBr, Cs₂CO₃, DMSO, 94%; (d) Fe, ammonium chloride, MeOH, H₂O, 90 °C, 86%; (e) LiOH, MeOH, H₂O, 75 °C, 93%; (f) formamidine acetate, MeOCH₂CH₂OH, 130 °C, 94%; (g) POCl₃, 120 °C, 3 h, 99%; (h) HNMe₂, DIPEA, IPA, 99%; (i) TFA, anisole, 75 °C, 65–95%; (j) di-*tert*-butylazodicarboxylate, triphenylphosphine, **18**, THF, 20–60%; (k) 3-(Et₂B)pyridine, Pd₂(dba)₃-CHCl₃, Cs₂CO₃, dioxane, 100 °C, 40–70%.

Scheme 6^a

^a Reaction conditions: (a) (MeO)₃CH, 105 °C; MeNH₂, toluene, 80 °C, 86% yield; (b) TFA, anisole, 75 °C, 95% yield; (c) di-*tert*-butylazodicarboxylate, triphenylphosphine, **18**, THF, r.t., 67% yield.

microsomal clearance of **26**, which would allow for potentially improved in vivo half-life, it was tested in the mouse CAR model, where clear efficacy was observed with an ED₅₀ = 3.2 mg/kg, sc, in wild type mice (Figure 11). No effect was seen in PDE10A knockout mice, which demonstrated that the efficacy in wild type mice was specific to PDE10A inhibition.^{4b}

Table 3. 4-Position Variations

	25	26	27
PDE10A IC ₅₀ (nM)	14	5	12
HLM, Cl _{int} (mL/min/kg)	178	<8	93
MDR BA/AB	0.9	1.5	0.6
MDR Papp, AB (× 10 ⁻⁶ cm/sec)	19	0.4	18
Mouse brain cGMP	268 ^a (32)	82 ^a (5.6)	129 ^b (32)
% increase (dose, mg/kg, sc)	34 ^a (5.6)		79 ^c (32)

^a Time of measurement: 60 min. ^b Time of measurement: 15 min. ^c Time of measurement: 30 min.

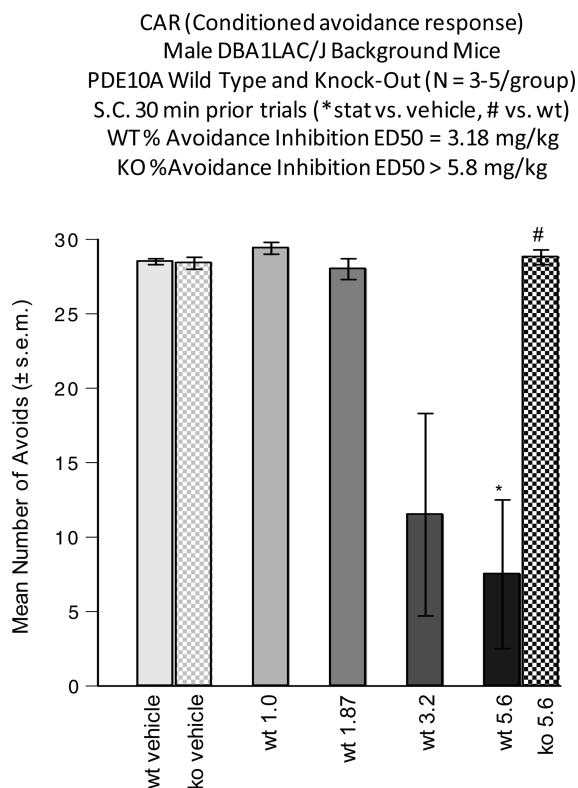


Figure 11. Conditioned avoidance responding study with compound 26 in wild type and PDE10A knockout mice.

In summary, we applied structure-based drug design to rationally hybridize the dual PDE10A/PDE3 inhibitor **1** with the highly selective inhibitor **2**, taking advantage of a selectivity pocket that is unique to PDE10A. Exploiting X-ray crystal structures, molecular modeling, and parallel chemistry, a series of quinoline and benzimidazole-based PDE10A inhibitors was identified that had significantly improved PDE3 selectivity. Utilizing the concept of ligand efficiency, the critical potency elements in the new series were identified, showing a significant change in previously observed SAR. This has resulted in a novel PDE10A lead class that accesses the selectivity pocket, broadly represented by multiple potent PDE10A inhibitors (**24**, **25**, **26**, **27**) with high ligand efficiency. Initial experiments have demonstrated *in vivo* increases in brain cGMP and efficacy in models predictive of antipsychotic activity. Furthermore, the ability to modulate *in vitro* permeability and clearance parameters has been demonstrated, suggesting that the further optimization of

these properties is possible to provide compounds with fully aligned potency, clearance, permeability, and efflux.

EXPERIMENTAL SECTION

Experimental Procedures. All reagents and solvents were used as purchased from commercial sources. Reactions were carried out under a blanket of nitrogen. Silica gel chromatography was done using the appropriate size Biotage prepacked silica filled cartridges. Mass spectral data was collected on a Micromass ADM atmospheric pressure chemical ionization instrument (LRMS APCI). NMR spectra were generated on a Varian 400 MHz instrument. Chemical shifts were recorded in ppm relative to tetramethylsilane (TMS) with multiplicities given as s (singlet), bs (broad singlet), d (doublet), t (triplet), dt (double of triplets), and m (multiplet). All compounds had purity of ≥95% as determined by high performance liquid chromatography (HPLC). HPLC conditions utilized are as follows: Waters Acuity UPLC: Mobile phase: A, acetonitrile with 0.1% formic acid; B, H₂O with 0.1% formic acid. Initial %A = 5%. Final %B = 100%. Gradient time = 1.2 min. Hold at 100% B for 0.3 min (1.5 min total). Compound identified by: ESI Positive mass spec; UV = 215 nm. Column = Waters CSH C18 1.7 μm 2.1 × 50 mm.

Chemistry Experimental Data. 4,5-Bis(4-methoxyphenyl)-2-(2-thienyl)-1H-imidazole (**2**). The title compound was synthesized according to the methods in ref 16. ¹H NMR (DMSO-*d*₆, 400 MHz) δ (ppm) = 7.59 (d, *J* = 3.7 Hz, 1H), 7.48 (d, *J* = 5 Hz, 1H), 7.35 (d, *J* = 8.3 Hz, 4H), 7.09 (t, m, 1H), 6.9 (m, 4H), 3.72 (s, 6H). ¹³C NMR (CDCl₃/CD₃OH) δ (ppm) = 159.08, 141.80, 133.17, 129.47, 127.70, 125.89, 125.30, 124.83, 113.93, 55.11. MS (APCI): 363.1 (M + H)⁺.

6,7-Dimethoxy-4-(3-phenylpiperidin-1-yl)quinazoline (**3**). 4-Chloro-6,7-dimethoxyquinazoline (15 g, 66.8 mmol) was mixed with 3-phenylpiperidine (11.8 g, 73.5 mmol) in isopropanol (300 mL), then diisopropylethylamine (23 mL, 133.6 mmol) was added and the mixture was heated at 90 °C for 2 h. After cooling to room temperature, the solvent was removed *in vacuo*, the residue was diluted with water and chloroform, and the mixture was made basic by adding sodium hydroxide (pH < 12). The mixture was extracted with chloroform; the organic layer was washed with brine and was dried over MgSO₄, was filtered, and was concentrated *in vacuo*. Purification by silica gel chromatography (100% chloroform to 100–1–1 chloroform/methanol/aq. conc. ammonium hydroxide) afforded 17.5 g (75% yield) of the title compound. ¹H NMR (CDCl₃, 400 MHz) δ (ppm) = 8.64 (s, 1H), 7.3 (m, 6H), 7.11 (s, 1H), 4.25 (m, 2H), 3.99 (s, 3H), 3.95 (s, 3H), 3.1 (m, 3H), 2.17 (m, 1H), 1.95 (m, 2H), 1.8 (m, 1H); ¹³C NMR (CDCl₃, 100 MHz) δ (ppm) = 164.34, 154.62, 153.36, 149.27, 148.58, 143.65, 128.84, 127.31, 127.00, 111.83, 107.67, 103.43, 57.08, 56.41, 56.17, 50.66, 43.20, 32.31, 25.97. MS (AP/CI): 350.2 (M + H)⁺.

7-Methoxy-4-(3-phenylpiperidin-1-yl)quinazolin-6-ol (**5**). Compound **3** (2.8 g, 8 mmol) was treated with L-methionine (1.43 g, 9.6 mmol) in methanesulfonic acid (40 mL). The mixture was heated to 120 °C for 2 h, 140 °C for 5 h, then 145 °C for 1 h. The mixture was poured onto ice, the pH was made basic by using sodium hydroxide (pH ~8–9), and the mixture was extracted with chloroform. The organic extracts were washed with brine, were dried over MgSO₄, were filtered, and were concentrated *in vacuo*. The residue was purified by silica gel chromatography (100–1–0 to 100–1–1 chloroform/methanol/conc. aq. ammonium hydroxide) to afford 1.4 g (52% yield) of the title compound. ¹H NMR (CDCl₃, 400 MHz) δ (ppm) = 8.63 (s, 1H), 7.33 (s, 1H), 7.27 (m, 4H), 7.19 (m, 3H), 4.3 (m, 1H), 3.95 (s, 3H), 3.0 (m, 2H), 2.9 (m, 1H), 2.07 (m, 1H), 1.75 (m, 3H); ¹³C NMR (CDCl₃, 100 MHz) δ (ppm) = 164.20, 153.26, 152.59, 147.96, 145.91, 143.56, 128.77, 127.32, 126.91, 112.41, 107.28, 106.84, 56.71, 56.39, 50.83, 42.96, 32.24, 25.93. MS (AP/CI): 336.2 (M + H)⁺.

7-Methoxy-4-(3-phenylpiperidin-1-yl)-6-propoxyquinazoline (7). Azadicarboxylic acid di-*tert*-butyl ester (280 mg, 1.2 mmol) in THF (5 mL) at 23 °C was treated with triphenylphosphine (395 mg, 1.49 mmol) and was stirred for 10 min. Compound 5 (200 mg, 0.6 mmol) was then added, followed by 1-propanol. After it was stirred for 24 h, the reaction mixture was diluted with ethyl acetate, was washed with saturated sodium bicarbonate solution, water, and brine, was dried over MgSO_4 , was filtered, and was concentrated in vacuo. The residue was purified by silica gel chromatography with ethyl acetate/methanol (100:1) to give 214 mg (95% yield) of the title compound. ^1H NMR (400 MHz, CDCl_3) δ (ppm) = 8.64 (s, 1H), 7.35–7.22 (m, 6H), 7.13 (s, 1H), 4.27–4.21 (2H, m), 4.1–4.0 (m, 2H), 3.98 (s, 3H), 3.15–3.02 (m, 3H), 2.16 (d, J = 11.9 Hz, 1H), 1.96–1.87 (m, 4H), 1.82 (m, 1H), 1.06 (t, J = 7.5 Hz, 3H); ^{13}C NMR (100 MHz, CDCl_3) δ (ppm) = 164.28, 154.99, 153.29, 149.15, 143.67, 128.81, 127.32, 126.99, 111.84, 107.70, 104.62, 70.79, 57.13, 56.37, 50.62, 43.29, 32.40, 26.00, 22.50, 10.67. MS (ES+): 378.6 (M + H)⁺.

7-Methoxy-4-(3-phenylpiperidin-1-yl)-6-(pyridin-2-ylmethoxy)quinazoline (8). A mixture of compound 5 (100 mg, 0.3 mmol), 2-picolyl chloride hydrochloride (74 mg, 0.45 mmol), and cesium carbonate (293 mg, 0.9 mmol) in DMSO (2 mL) was stirred at 23 °C for 6 h. The mixture was diluted with 5% *n*-butanol in ethyl acetate and was washed with water and then brine, was dried over MgSO_4 , was filtered, and was concentrated in vacuo. Purification by silica gel chromatography (200:1:2 CHCl_3 –MeOH– NH_4OH (aq)) gave 109 mg (85%) of the title compound. ^1H NMR (400 MHz, CDCl_3) δ (ppm) = 8.6 (s, 1H), 8.5 (d, J = 4.6 Hz, 1H), 7.58 (m, 1H), 7.48 (d, J = 7.9 Hz, 1H), 7.2 (m, 5H), 7.08 (m, 1H), 5.4 (d, J = 14.0 Hz, 1H), 5.3 (d, J = 13.7, 1H), 4.1 (dd, J = 1.7, 11.2 Hz, 1H), 4.0 (s, 3H), 3.96 (m, 1H), 3.0 (m, 3H), 2.07 (d, J = 12.0 Hz, 1H), 1.8 (m, 3H); ^{13}C NMR (100 MHz, CDCl_3) δ (ppm) = 164.24, 156.67, 154.85, 153.45, 149.47, 149.34, 146.95, 143.75, 137.08, 128.77, 127.44, 126.88, 123.03, 121.49, 111.62, 107.85, 106.18, 71.82, 56.62, 56.44, 50.88, 42.97, 32.22, 25.89. MS (AP/CI): 427.3 (M + H)⁺.

Compounds 9–11. All were prepared in a manner analogous to compound 8 via alkylation of compound 5 with the appropriate alkyl halide.

7-Methoxy-4-(3-phenylpiperidin-1-yl)-6-(pyridin-3-ylmethoxy)quinazoline (9). The title compound was obtained in 84% yield (107 mg) following silica gel chromatography. ^1H NMR (CDCl_3 , 400 MHz) δ (ppm) = 8.68 (d, J = 1.2 Hz, 1H), 8.62 (s, 1H), 8.5 (m, 1H), 7.75 (ddd, J = 1.7, 2.1, 7.9 Hz, 1H), 7.25 (m, 8H), 7.11 (s, 1H), 5.20 (s, 2H), 4.16 (m, 1H), 4.04 (d, J = 13.7 Hz, 1H), 3.98 (s, 3H), 3.0 (m, 3H), 2.1 (m, 1H), 1.8 (m, 3H); ^{13}C NMR (CDCl_3 , 100 MHz) δ (ppm) = 164.21, 155.06, 153.60, 149.91, 149.60, 148.99, 146.90, 143.65, 135.27, 131.99, 128.85, 127.36, 127.01, 123.82, 111.45, 108.05, 106.69, 68.92, 56.68, 56.42, 50.82, 43.07, 32.31, 25.93. MS (AP/CI): 427.2 (M + H)⁺.

7-Methoxy-4-(3-phenylpiperidin-1-yl)-6-(pyridin-4-ylmethoxy)quinazoline (10). The title compound was obtained in 85% yield (108 mg) following silica gel chromatography. ^1H NMR (CDCl_3 , 400 MHz) δ (ppm) = 8.62 (s, 1H), 8.57 (d, J = 1.7 Hz, 2H), 7.3 (m, 5H), 7.24 (m, 4H), 7.04 (s, 1H), 5.21 (d, J = 2.1 Hz, 2H), 4.18 (dt, J = 1.7, 12.9 Hz, 1H), 4.02 (s, 3H), 3.95 (m, 1H), 3.06 (m, 1H), 2.95 (m, 2H), 2.1 (m, 1H), 1.75 (m, 3H). ^{13}C NMR (CDCl_3 , 100 MHz), δ (ppm) = 164.20, 154.96, 153.62, 150.42, 149.56, 146.74, 145.58, 143.61, 128.86, 127.32, 127.03, 121.45, 111.40, 108.10, 106.51, 69.50, 56.47, 50.97, 42.98, 32.33, 25.97. MS (AP/CI): 427.3 (M + H)⁺.

7-Methoxy-4-(3-phenylpiperidin-1-yl)-6-(quinolin-2-ylmethoxy)quinazoline (11). The title compound was obtained in 80% yield (115 mg) following silica gel chromatography. ^1H NMR (400 MHz, CDCl_3) δ (ppm) = 8.57 (s, 1H), 8.1 (m, 2H), 7.76 (m, 1H), 7.72 (m, 1H), 7.65 (d, J = 8.7 Hz, 1H), 7.25 (m, 6H), 7.18 (s, 1H), 5.59 (d, J = 13.7 Hz, 1H), 5.54 (d, J = 14.1 Hz, 1H), 4.16 (m, 1H), 4.03 (s, 1H), 3.8 (m, 2H), 3.0–2.8 (m, 3H), 2.02 (m, 1H), 1.7 (m, 2H), 1.5 (m, 1H); ^{13}C NMR

(100 MHz, CDCl_3) δ (ppm) = 25.9, 32.1, 42.7, 51.0, 56.5, 72.6, 77.5, 106.3, 107.7, 111.6, 119.1, 126.9, 127.0, 127.4, 127.8, 128.1, 128.8, 129.0, 130.1, 137.5, 143.8, 147.0, 147.8, 149.1, 153.4, 154.8, 157.5, 164.2. MS (AP/CI): 477.3 (M + H)⁺.

Compounds 12–15, 19, and 20. All were prepared using a procedure analogous to that used to prepare compound 16 via Mitsunobu alkylation of compound 5 with the appropriate alkyl alcohol

7-Methoxy-6-(2-phenylethoxy)-4-(3-phenylpiperidin-1-yl)quinazoline (12). The title compound was obtained in 85% yield (75 mg). ^1H NMR (400 MHz, CDCl_3) δ (ppm) = 8.65 (s, 1H), 7.4–7.2 (m, 11H), 7.13 (s, 1H), 4.33–4.19 (m, 4H), 3.99 (s, 3H), 3.28 (t, J = 7.5 Hz, 2H), 3.19–2.97 (m, 3H), 2.11 (m, 1H), 1.95–1.77 (m, 3H); ^{13}C NMR (100 MHz, CDCl_3) δ (ppm) = 164.32, 154.99, 153.38, 149.29, 147.78, 143.60, 137.79, 129.31, 128.89, 128.83, 127.31, 127.00, 111.77, 107.80, 104.97, 70.03, 57.33, 56.41, 50.42, 43.25, 35.84, 32.33, 25.97. MS (AP/CI): 440.2 (M + H)⁺.

7-Methoxy-4-(3-phenylpiperidin-1-yl)-6-(2-pyridin-2-ylethoxy)quinazoline (13). The title compound was obtained in 80% yield (70 mg). ^1H NMR (400 MHz, CDCl_3) δ (ppm) = 8.63 (s, 1H), 8.57 (m, 1H), 7.63 (m, 1H), 7.23–7.15 (m, 9H), 4.5 (m, 2H), 4.2 (m, 2H), 3.96 (s, 3H), 3.80 (m, 2H), 3.05 (m, 3H), 2.1 (m, 1H), 1.9 (m, 2H), 1.8 (m, 1H); ^{13}C NMR (100 MHz, CDCl_3) δ (ppm) = 26.0, 32.2, 37.9, 43.2, 50.6, 56.4, 57.3, 68.5, 105.3, 107.7, 111.8, 122.0, 124.1, 126.9, 127.4, 128.8, 136.7, 143.7, 147.8, 149.3, 149.7, 153.3, 155.0, 158.2, 164.3. MS (AP/CI): 441.1 (M + H)⁺.

7-Methoxy-4-(3-phenylpiperidin-1-yl)-6-(2-pyridin-3-ylethoxy)quinazoline (14). The title compound was obtained in 70% yield (62 mg). ^1H NMR (400 MHz, CDCl_3) δ (ppm) = 8.63 (s, 1H), 8.58 (s, 1H), 8.5 (d, J = 4.1 Hz, 1H), 7.65 (m, 1H), 7.3–7.2 (m, 7H), 4.3–4.15 (m, 4H), 3.97 (s, 3H), 3.18 (m, 2H), 3.07 (m, 2H), 2.98 (m, 1H), 2.12 (m, 1H), 1.95–1.72 (m, 3H); ^{13}C NMR (100 MHz, CDCl_3) δ (ppm) = 164.22, 155.01, 153.32, 150.62, 149.22, 148.46, 147.58, 143.55, 136.88, 133.63, 128.84, 127.27, 127.04, 123.68, 111.54, 107.76, 105.24, 69.35, 57.12, 56.40, 50.51, 43.21, 33.05, 32.32, 25.95. MS (AP/CI): 441 (M + H)⁺.

7-Methoxy-4-(3-phenylpiperidin-1-yl)-6-(2-pyridin-4-ylethoxy)quinazoline (15). The title compound was obtained in 64% yield (56 mg). ^1H NMR (400 MHz, CDCl_3) δ (ppm) = 8.63 (s, 1H), 8.53 (d, J = 5.8 Hz, 1H), 7.3–7.2 (m, 9H), 7.10 (s, 1H), 4.3–4.2 (m, 4H), 3.96 (m, 3H), 3.17 (m, 2H), 3.07 (m, 2H), 2.98 (m, 1H), 2.13 (m, 1H), 1.95–1.75 (m, 3H); ^{13}C NMR (100 MHz, CDCl_3) δ (ppm) = 164.20, 155.02, 153.36, 150.16, 149.27, 147.50, 147.10, 143.54, 128.84, 127.26, 127.04, 124.61, 111.51, 107.81, 105.50, 68.76, 57.11, 56.39, 50.49, 43.19, 35.11, 32.36, 25.94. MS (AP/CI): 441.3 (M + H)⁺.

7-Methoxy-4-(3-phenylpiperidin-1-yl)-6-(2-quinolin-2-ylethoxy)quinazoline (16). Di-*tert*-butyl azodicarboxylate (92 mg, 0.4 mmol) was mixed with triphenylphosphine (131 mg, 0.5 mmol) in THF (2 mL) at room temperature for 10 min. Compound 5 (67 mg, 0.2 mmol) was added followed by 2-(quinolin-2-yl)ethanol (138 mg, 0.8 mmol), and the solution was stirred at room temperature for 24 h. The reaction mixture was diluted with ethyl acetate, was washed with aqueous sodium bicarbonate, water, and then brine, was dried over MgSO_4 , was filtered, and was concentrated in vacuo. The residue was dissolved in methylene chloride and was applied to a column packed with silica-bound *p*-toluene sulfonic acid. The column was eluted by gravity with 2 column volumes (cv) of methylene chloride, 3 cv of methanol to remove reaction byproduct, then was eluted with 4 cv of 1 N triethylamine in methanol to remove the product. The solvent from the triethylamine elution was removed in vacuo and the resulting residue was purified by silica gel chromatography (50–1–0 to 50–1–1 chloroform/methanol; 50–1 chloroform/triethylamine) to afford the title compound in 30% yield. ^1H NMR (400 MHz, CDCl_3) δ (ppm) = 8.63 (s, 1H), 8.10 (d, J = 8.3 Hz, 1H), 8.05 (d, J = 8.7 Hz, 1H), 7.80 (d, J = 7.9 Hz, 1H), 7.7 (m, 1H), 7.51 (t, J = 7.47 Hz, 1H), 7.43 (d, J = 8.3 Hz, 1H), 7.2 (m, 7H), 4.6 (m, 2H),

4.23 (m, 2H), 3.97 (s, 3H), 3.58 (m, 2H), 3.04 (m, 3H), 2.11 (m, 1H), 1.9 (m, 2H), 1.75 (m, 1H); ^{13}C NMR (100 MHz, CDCl_3) δ (ppm) = 26.0, 32.3, 38.7, 43.2, 50.7, 56.4, 57.1, 68.6, 105.4, 107.8, 111.8, 122.4, 126.3, 126.9, 127.2, 127.3, 127.8, 128.8, 129.1, 129.8, 136.6, 143.7, 153.4, 155.0, 158.9, 164.3. MS (AP/CI): 491.1 ($\text{M} + \text{H}$) $^+$.

7-Methoxy-6-[3-(1-methyl-1H-benzimidazol-2-yl)propoxy]-4-(3-phenylpiperidin-1-yl)quinazoline (19). The title compound was prepared in 49% yield. ^1H NMR (400 MHz, CD_3OD) δ (ppm) = 8.45 (s, 1H), 7.58 (m, 1H), 7.34 (m, 1H), 7.27–7.14 (m, 7H), 7.12 (s, 1H), 7.09 (s, 1H), 4.3–4.1 (m, 4H), 3.87 (s, 3H), 3.74 (s, 3H), 3.14 (m, 4H), 2.98 (m, 1H), 2.42 (m, 2H), 2.1 (m, 1H); ^{13}C NMR (100 MHz, CD_3OD) δ (ppm) = 163.84, 155.48, 154.67, 152.03, 147.97, 147.75, 143.31, 141.48, 135.63, 128.67, 127.10, 126.89, 122.65, 122.40, 118.11, 111.00, 109.65, 105.89, 105.06, 67.80, 56.62, 55.86, 50.43, 43.10, 32.15, 29.59, 26.94, 25.79, 23.69. MS (AP/CI): 508 ($\text{M} + \text{H}$) $^+$.

2-[2-(Isoquinolin-7-yloxy)ethyl]quinoline (20). The title compound was prepared in 21% yield. ^1H NMR (400 MHz, CDCl_3) δ (ppm) = 9.11 (s, 1H), 8.38 (d, J = 5.8 Hz, 1H), 8.11 (d, J = 8.3 Hz, 1H), 8.07 (d, J = 8.3 Hz, 1H), 7.79 (d, J = 8.3 Hz, 1H), 7.75–7.68 (m, 2H), 7.56 (d, J = 5.8 Hz, 1H), 7.5 (m, 1H), 7.43 (d, J = 8.3 Hz, 1H), 7.32 (dd, J = 2.5, 9.1 Hz, 1H), 7.26 (s, 1H), 4.61 (t, J = 6.6 Hz, 2H), 3.54 (t, J = 6.6 Hz, 2H); ^{13}C NMR (100 MHz, CDCl_3) δ (ppm) = 159.00, 157.91, 150.95, 140.87, 136.82, 131.77, 129.92, 128.96, 128.26, 127.82, 127.23, 126.41, 124.27, 122.22, 120.68, 109.01, 106.07, 67.66, 38.72. MS (AP/CI): 301.3 ($\text{M} + \text{H}$) $^+$.

6,7-Dimethoxyquinazoline (22). A mixture of 2,4-dichloro-6, 7-dimethoxyquinazoline (5 g, 19.3 mmol), triethylamine (5.6 mL), and palladium on carbon (10%, 0.5 g) in methanol (200 mL) was shaken under hydrogen (40 psi) at room temperature for 26 h. The mixture was filtered through Celite, was concentrated in vacuo, and was purified by silica gel chromatography (chloroform–methanol 100:1) to afford 2.4 g (65% yield) of the title compound. ^1H NMR (400 MHz, CDCl_3) δ (ppm) = 9.11 (s, 1H), 9.10 (s, 1H), 7.27 (s, 1H), 7.06 (s, 1H), 4.02 (s, 3H), 4.00 (s, 3H); ^{13}C NMR (100 MHz, CDCl_3) δ (ppm) = 156.86, 156.49, 154.16, 150.89, 148.20, 121.26, 106.71, 104.00, 56.67, 56.46; MS (AP/CI): 191.1 ($\text{M} + \text{H}$) $^+$.

6-Methoxyquinazolin-7-ol (23). 6,7-Dimethoxyquinazoline (compound 22, 2.3 g, 12 mmol) and L-methionine (2.1 g, 14.4 mmol) in methanesulfonic acid (60 mL) was heated as follows: 120 °C, 1 h; 140 °C, 2 h; 145 °C, 4 h; 120 °C, 16 h. More L-methionine (0.5 g) was added, and the mixture was heated at 145 °C for 6 h and 120 °C for 16 h. After cooling to room temperature, the mixture was poured onto ice, the pH was adjusted to 7–8 with sodium hydroxide, and the aqueous mixture was extracted using chloroform in a “heavier-than-water” continuous extraction device for 72 h. The chloroform was then concentrated in vacuo and the residue was purified by silica gel chromatography (chloroform–methanol 50:1) to afford 1.2 g (57% yield) of the title compound. ^1H NMR (400 MHz, $\text{CD}_3\text{OD}/\text{CDCl}_3$) δ (ppm) = 9.09 (s, 1H), 8.91 (s, 1H), 7.24 (s, 1H), 7.22 (s, 1H), 4.01 (s, 3H); ^{13}C NMR (100 MHz, $\text{CD}_3\text{OD}/\text{CDCl}_3$) δ (ppm) = 156.69, 156.12, 152.46, 150.95, 147.84, 121.07, 108.63, 104.57, 56.02. MS (AP/CI): 177.2 ($\text{M} + \text{H}$) $^+$.

6-Methoxy-7-(2-quinolin-2-ylethoxy)quinazoline (24). Azadicarboxylic acid ditert-butyl ester (267 mg, 1.14 mmol) in THF (5 mL) at 23 °C was treated with triphenylphosphine (376 mg, 1.42 mmol) and was stirred for 10 min. Compound 23 (100 mg, 0.57 mmol) was then added, followed by 2-(quinolin-2-yl)ethanol (394 mg, 2.3 mmol). After stirring for 24 h, the reaction mixture was diluted with ethyl acetate, was washed with saturated sodium bicarbonate solution, water, and brine. The organic layer was then dried over MgSO_4 , was filtered, and was concentrated in vacuo. The residue was purified by silica gel chromatography (50:1 to 20:1 ethyl acetate–methanol) to afford 180 mg (95% yield) of the title compound. ^1H NMR (400 MHz, CDCl_3) δ (ppm) = 9.104 (s, 1H), 9.097 (s, 1H), 8.08 (d, J = 8.3 Hz, 1H), 8.04 (d, J = 8.3 Hz, 1H), 7.76 (m, 1H), 7.67 (m, 1H), 7.47 (m, 1H), 7.42 (d, J = 8.7 Hz, 1H), 7.38 (s, 1H), 7.03 (s, 1H), 4.71 (t, J = 7.1 Hz, 2H), 3.96 (s, 3H), 3.59 (t,

J = 7.1 Hz, 2H); ^{13}C NMR (100 MHz, CDCl_3) δ (ppm) = 158.49, 156.83, 155.80, 154.19, 151.10, 148.18, 148.05, 136.74, 129.85, 129.07, 127.75, 127.20, 126.39, 122.23, 121.25, 112.50, 107.64, 104.14, 68.53, 56.41, 38.15. MS (AP/CI): 332.2 ($\text{M} + \text{H}$) $^+$.

Preparation of Key Intermediates in Scheme 5 Toward Preparation of Compounds 25A and 26A. **Step A: 5-Hydroxy-4-methoxy-2-nitrobenzoic Acid.** A mixture of 4,5-dimethoxy-2-nitrobenzoic acid (15 g, 66 mmol) in aqueous sodium hydroxide (6 M, 60 mL) was heated at 100 °C for 3 h, was cooled to room temperature, and was poured into a mixture of concentrated hydrochloric acid and crushed ice (pH < 2). The mixture was extracted with ethyl acetate, was washed with brine, was dried over MgSO_4 , was filtered, and was concentrated in vacuo to afford 14 g (99% yield) of the title compound. ^1H NMR (400 MHz, CD_3OD) δ (ppm) = 7.55 (s, 1H), 7.06 (s, 1H), 3.95 (s, 3H); ^{13}C NMR (100 MHz, CD_3OD) δ (ppm) = 55.82, 107.46, 114.98, 122.90, 140.33, 149.09, 151.13, 167.96. MS (AP/CI): 212 ($\text{M} - \text{H}$) $^-$.

Step B: Methyl-5-hydroxy-4-methoxy-2-nitrobenzoate. 5-Hydroxy-4-methoxy-2-nitrobenzoic acid (15 g, 70.4 mmol) in methanol (100 mL) was treated with concentrated sulfuric acid (10 mL). The mixture was heated at reflux for 48 h. After cooling to room temperature, the methanol was removed under reduced pressure, the resulting residue was diluted with water and was extracted with ethyl acetate. The organic layer was washed with water and then brine, was dried over MgSO_4 , was filtered, and was concentrated to afford 15.4 g (96% yield) of the title compound. ^1H NMR (400 MHz, CD_3OD) δ (ppm) = 7.56 (s, 1H), 6.99 (s, 1H), 3.95 (s, 3H), 3.84 (s, 3H); ^{13}C NMR (100 MHz, CD_3OD) δ (ppm) = 166.89, 151.53, 149.18, 122.39, 114.88, 107.59, 55.85, 52.32. MS (AP/CI): 228 ($\text{M} + \text{H}$) $^+$; 226 ($\text{M} - \text{H}$) $^-$.

Step C: Methyl 5-(benzyloxy)-4-methoxy-2-nitrobenzoate. Methyl-5-hydroxy-4-methoxy-2-nitrobenzoate (15.4 g, 68 mmol), benzyl bromide (9.7 mL, 82 mmol), and cesium carbonate (44 g, 136 mmol) in DMSO (200 mL) were stirred at room temperature for 24 h. The mixture was diluted with ethylacetate (~2 L) and *n*-butanol (~100 mL). The mixture was washed with water and brine, was dried over MgSO_4 , was filtered, and was concentrated. The residue was purified by silica gel chromatography (1:5 to 2:1 ethylacetate–hexanes) to afford 20.2 g (94% yield) of the title compound. ^1H NMR (400 MHz, CDCl_3) δ (ppm) = 7.44–7.32 (m, 6H), 7.14 (s, 1H), 5.19 (s, 2H), 3.94 (s, 3H), 3.88 (s, 3H); ^{13}C NMR (100 MHz, CDCl_3) δ (ppm) = 166.35, 151.83, 151.19, 135.40, 129.04, 128.78, 127.75, 121.48, 112.86, 107.49, 71.65, 56.79, 53.42. MS (AP/CI): 286.1 ($\text{M} + \text{H}$) $^+$.

Step D: Methyl 2-Amino-5-(benzyloxy)-4-methoxybenzoate. Methyl 5-(benzyloxy)-4-methoxy-2-nitrobenzoate (20 g, 63 mmol) was mixed with ammonium chloride (50.6 g, 945 mmol) in methanol (200 mL) and water (50 mL), then iron powder (35.3 g, 630 mmol) was added and the mixture was heated at 90 °C for 24 h. The mixture was filtered while hot through Celite, and the filter cake was washed with methylene chloride and water. The aqueous and organic layers were separated and the aqueous layer was made basic with sodium bicarbonate and was extracted with methylene chloride. The organic layers were combined and were washed with brine, were dried over MgSO_4 , were filtered, and were concentrated to afford 15.5 g (86% yield) of the title compound. ^1H NMR (400 MHz, CDCl_3) δ (ppm) = 7.46–7.26 (m, 6H), 6.15 (s, 1H), 5.02 (s, 2H), 3.84 (s, 3H), 3.82 (s, 3H). MS (AP/CI): 288.2 ($\text{M} + \text{H}$) $^+$.

Step E: 2-Amino-5-(benzyloxy)-4-methoxybenzoic Acid. Methyl 2-amino-5-(benzyloxy)-4-methoxybenzoate (15.5 g, 54 mmol) was treated with lithium hydroxide (13 g, 540 mmol) in methanol/water/THF (1:1:2, 60 mL total volume). The mixture was heated at 75 °C for 6 h. After the mixture was cooled, the methanol and THF were removed in vacuo, and the aqueous layer was diluted with water, the pH was adjusted to ~7 by using 1 N HCl, and the aqueous layer was extracted with ethyl acetate. The organic layer was washed with brine, was dried over MgSO_4 , was filtered, and was concentrated to afford 13.7 g (93% yield) of the title compound. ^1H NMR (400 MHz, $\text{CD}_3\text{OD}/\text{CDCl}_3$) δ (ppm) = 7.40

(s, 1H), 7.33–7.23 (m, 6H), 6.27 (s, 1H), 4.97 (s, 2H), 4.7 (br s, 2H), 3.81 (s, 3H); ^{13}C NMR (100 MHz, $\text{CD}_3\text{OD}/\text{CDCl}_3$) δ (ppm) = 140.0, 137.32, 128.47, 128.40, 127.98, 127.35, 127.00, 117.81, 99.93, 72.62, 55.58. MS (AP/CI): 274.2 (M + H) $^+$.

Step F: 6-(Benzyloxy)-7-methoxyquinazolin-4(3H)-one. 2-Amino-5-(benzyloxy)-4-methoxybenzoic acid (5 g, 18.3 mmol) was mixed with amidine acetate (3.8 g, 36.6 mmol) in ethylene glycol monomethyl ether (25 mL) and the mixture was heated at 130 °C for 24 h. After it was cooled to room temperature, part of the solvent was removed in vacuo and ammonium hydroxide (5 mL, 30% in water) and water (50 mL) were added. The solid was filtered, was washed with water and hexanes, and was then dried under vacuum to afford 4.87 g (94% yield) of the title compound. ^1H NMR (400 MHz, $\text{CD}_3\text{OD}/\text{CDCl}_3$) δ (ppm) = 7.91 (s, 1H), 7.63 (s, 1H), 7.55 (s, 1H), 7.45 (m, 2H), 7.35 (m, 2H), 7.3 (m, 1H), 7.10 (s, 1H), 5.21 (s, 2H), 3.98 (s, 3H); ^{13}C NMR characteristic peaks ($\text{CD}_3\text{OD}/\text{CDCl}_3$) δ (ppm) = 156.04, 148.67, 143.52, 136.21, 128.67, 128.26, 127.74, 107.55, 107.24, 71.09, 56.17. MS (AP/CI): 283.1 (M + H) $^+$.

Step G: 6-(Benzyloxy)-4-chloro-7-methoxyquinazolin-4(3H)-one (4.85 g, 17.2 mmol) in phosphorus oxychloride (25 mL) was heated to 120 °C for 3 h. After cooling to room temperature, the phosphorus oxychloride was removed in vacuo, the residue was slowly added to saturated aqueous potassium carbonate and the mixture was stirred until bubbling ceased. The aqueous mixture was extracted with chloroform, the organic layer was washed with brine, was dried over MgSO_4 , was filtered, and was concentrated to afford 5.1 g (99% yield) of the title compound. ^1H NMR (400 MHz, CDCl_3) δ (ppm) = 8.85 (s, 1H), 7.50 (m, 2H), 7.45 (m, 4H), 5.29 (s, 2H), 4.05 (s, 3H); ^{13}C NMR (100 MHz, CDCl_3) δ (ppm) = 159.64, 157.68, 152.31, 150.84, 148.61, 135.55, 129.04, 128.75, 127.90, 119.67, 106.76, 104.62, 71.47, 56.95. MS (AP/CI): 301.1, 303.1 (M + H) $^+$.

Step H: 6-(Benzyloxy)-7-methoxy-N,N-dimethylquinazolin-4-amine. A solution of 6-(benzyloxy)-4-chloro-7-methoxyquinazolin-4-amine (500 mg, 1.66 mmol), dimethylamine (8.3 mL of 2 M solution in methanol, 16.6 mmol), and diisopropylethyl amine (580 μL , 3.32 mmol) in isopropanol (10 mL) was heated at 90 °C for 4 h. The solvent was removed in vacuo, the residue was diluted with water and chloroform, and the pH was adjusted to >12 using 1 N sodium hydroxide. The biphasic mixture was extracted with chloroform, the organic layer was washed with brine, was dried over MgSO_4 , was filtered, and was concentrated. Purification by silica gel chromatography (chloroform–methanol, 75:1) gave 440 mg (86% yield) of the title compound. ^1H NMR (400 MHz, CDCl_3) δ (ppm) = 8.52 (s, 1H), 7.44 (m, 2H), 7.36 (m, 2H), 7.28 (m, 1H), 7.21 (s, 1H), 7.17 (s, 1H), 5.26 (s, 2H), 4.01 (s, 3H), 3.06 (s, 6H); ^{13}C NMR (100 MHz, CDCl_3) δ (ppm) = 163.26, 154.77, 153.14, 149.25, 146.30, 136.60, 128.97, 128.28, 127.18, 110.39, 107.94, 107.73, 71.46, 56.34, 41.66. MS (AP/CI): 310.1 (M + H) $^+$.

Step I: 4-(Dimethylamino)-7-methoxyquinazolin-6-ol. 6-(Benzyloxy)-7-methoxy-N,N-dimethylquinazolin-4-amine (410 mg, 1.33 mmol) and anisole (2.9 mL, 26.6 mmol) in trifluoroacetic acid (25 mL) were heated at 75 °C for 24 h. The solvent was removed in vacuo and the residue was purified by silica gel chromatography (chloroform–methanol, 10:1) to afford the title compound in 99% yield (290 mg). ^1H NMR (400 MHz, $\text{CD}_3\text{OD}/\text{CDCl}_3$) δ (ppm) = 8.40 (s, 1H), 7.59 (s, 1H), 7.23 (s, 1H), 4.02 (s, 3H), 3.56 (s, 6H); ^{13}C NMR (100 MHz, $\text{CD}_3\text{OD}/\text{CDCl}_3$) δ (ppm) = 161.27, 155.87, 147.37, 145.60, 136.02, 110.07, 107.36, 99.55, 56.51, 42.36. MS (AP/CI): 220.2 (M + H) $^+$.

7-Methoxy-N,N-dimethyl-6-(2-quinolin-2-ylethoxy)quinazolin-4-amine (25). Following the procedure for compound 16 using 4-(dimethylamino)-7-methoxyquinazolin-6-ol as starting material, the desired product was obtained in 32% yield (86 mg) following silica gel chromatography. ^1H NMR (400 MHz, CDCl_3) δ (ppm) = 8.52 (s, 1H), 8.07 (d, J = 8.3 Hz, 1H), 8.01 (d, J = 8.3 Hz, 1H), 7.76 (d, J = 7.9 Hz, 1H), 7.67 (m, 1H), 7.48 (m, 1H), 7.42 (d, J = 8.3 Hz, 1H), 7.29 (s, 1H), 7.16 (s, 1H), 4.59 (t, i = 7.1 Hz, 2H), 3.94 (s, 3H), 3.53 (t, J = 7.1 Hz,

2H), 3.20 (s, 6H); ^{13}C NMR (100 MHz, CDCl_3) δ (ppm) = 163.35, 158.99, 154.66, 153.09, 149.23, 148.20, 146.93, 136.63, 129.76, 129.02, 127.83, 127.20, 126.31, 122.4, 110.61, 107.69, 106.78, 68.89, 6.26, 41.90, 38.77. MS (AP/CI): 375.3 (M + H) $^+$.

Step K: 6-(Benzyloxy)-7-methoxy-4-(pyridin-3-yl)quinazolin-4(3H)-one. 6-(Benzyloxy)-4-chloro-7-methoxyquinazolin-4(3H)-one (1 g, 3.3 mmol) was mixed with 3-(1,3,2-dioxaborinan-2-yl)pyridine (0.65 g, 4 mmol), $\text{Pd}_2(\text{dba})_3\text{-CHCl}_3$ (72 mg, 0.07 mmol), tricyclohexyl phosphine (56 mg, 0.2 mmol), and cesium carbonate (1.6 g, 5 mmol) in dioxane (10 mL). The mixture was heated to 100 °C for 24 h, was cooled to room temperature, was concentrated in vacuo, was diluted with 1 N sodium hydroxide and water (1:1), and was extracted with chloroform, and the organic layer was washed with brine and was dried over MgSO_4 , was filtered, and was concentrated in vacuo. Purification by silica gel chromatography (ethyl acetate–hexanes–methanol 8:1:0 to 8:1:0.5) afforded 1 g (88% yield) of the title compound. ^1H NMR (400 MHz, CDCl_3) δ (ppm) = 9.17 (s, 1H), 8.90 (d, J = 1.7 Hz, 1H), 8.78 (dd, J = 1.7, 5.0 Hz, 1H), 7.82 (dt, J = 2.1, 7.9 Hz, 1H), 7.43–7.31 (m, 6H), 7.20 (s, 1H), 5.19 (s, 2H), 4.08 (s, 3H); ^{13}C NMR (100 MHz, CDCl_3) δ (ppm) = 162.09, 156.73, 153.85, 150.82, 150.40, 149.76, 149.51, 137.19, 135.94, 133.67, 129.04, 128.55, 127.48, 123.71, 118.81, 107.50, 105.74, 71.18, 56.72. MS (AP/CI): 344.1 (M + H) $^+$.

Step I: 7-Methoxy-4-(pyridin-3-yl)quinazolin-6-ol. 6-(Benzyloxy)-7-methoxy-4-(pyridin-3-yl)quinazolin-4(3H)-one (1 g, 2.9 mmol) and anisole (6.3 g, 58 mmol) in trifluoroacetic acid (40 mL) was heated at 75 °C for 24 h. After the mixture was cooled to room temperature and concentration in vacuo, the residue was purified by silica gel chromatography (chloroform–methanol, 30:1) to afford 0.73 g (99% yield) of the title compound. ^1H NMR (400 MHz, $\text{CD}_3\text{OD}/\text{CDCl}_3$) δ (ppm) = 9.07 (s, 1H), 8.96 (d, J = 1.7 Hz, 1H), 8.77 (dd, J = 1.7, 5.0 Hz, 1H), 8.31 (m, 1H), 7.73 (dd, J = 5.0, 7.9 Hz, 1H), 7.39 (s, 1H), 7.27 (s, 1H), 4.09 (s, 3H); ^{13}C NMR (100 MHz, $\text{CD}_3\text{OD}/\text{CDCl}_3$) δ (ppm) = 161.07, 156.88, 151.64, 149.92, 149.05, 148.44, 148.03, 139.51, 134.29, 124.71, 119.62, 106.54, 105.88, 56.34. MS (AP/CI): 254.1 (M + H) $^+$.

7-Methoxy-4-pyridin-3-yl-6-(2-quinolin-2-ylethoxy)quinazolin-4(3H)-one (26). Following the procedure for compound 16 using 7-methoxy-4-(pyridin-3-yl)quinazolin-6-ol as starting material, the title compound was obtained in 63% yield. ^1H NMR (400 MHz, CDCl_3) δ (ppm) = 9.17 (s, 1H), 8.99 (brs, 1H), 8.74 (brs, 1H), 8.06 (m, 2H), 7.96 (d, J = 8.3 Hz, 1H), 7.76 (d, J = 7.9 Hz, 1H), 7.66 (m, 1H), 7.47 (m, 2H), 7.40 (d, J = 8.7, 1H), 7.35 (s, 1H), 7.28 (s, 1H), 4.52 (t, J = 6.6 Hz, 2H), 4.01 (s, 3H), 3.52 (t, J = 6.6 Hz, 2H); ^{13}C NMR (100 MHz, CDCl_3) δ (ppm) = 38.5, 56.6, 68.6, 104.6, 107.4, 119.0, 122.3, 123.9, 126.4, 127.2, 127.8, 129.0, 129.8, 133.8, 136.7, 137.2, 148.1, 149.5, 150.3, 150.4, 150.9, 153.8, 156.6, 158.5, 162.1. MS (AP/CI): 409.0 (M + H) $^+$.

Preparation of Key Intermediates in Scheme 6 Toward Preparation of Compound 27.

Step A: 6-(Benzyloxy)-7-methoxy-3-methylquinazolin-4(3H)-one. A solution of 2-amino-5-(benzyloxy)-4-methoxybenzoic acid (Scheme 5, Step E) (100 mg, 0.37 mmol) in trimethyl orthoformate (1 mL, 9 mmol) was heated at 105 °C for 2 h. The solvent was removed in vacuo, dry toluene was added, followed by methylamine (2 M in THF, 1.83 mL). The mixture was heated to 80 °C for 24 h, the solvent was removed in vacuo, and the residue was purified by silica gel chromatography (ethyl acetate–methanol, 50:1) to afford 99 mg (91% yield) of the title compound. ^1H NMR (400 MHz, CDCl_3) δ (ppm) = 7.94 (s, 1H), 7.68 (s, 1H), 7.47 (m, 2H), 7.38–7.25 (m, 3H), 7.09 (s, 1H), 5.23 (s, 2H), 3.97 (s, 3H), 3.55 (s, 3H); ^{13}C NMR (100 MHz, CDCl_3) δ (ppm) = 161.12, 155.50, 148.69, 145.82, 144.88, 136.36, 128.86, 128.36, 127.79, 115.50, 108.20, 107.45, 71.19, 56.47, 34.28. MS (ES $^+$): 297.5 (M + H) $^+$.

Step B: 6-Hydroxy-7-methoxy-3-methylquinazolin-4(3H)-one. 6-(Benzyloxy)-7-methoxy-3-methylquinazolin-4(3H)-one was converted to the title compound in 95% yield (58 mg) using the debenzoylation conditions as detailed for Scheme 5, Step I. ^1H NMR (400 MHz,

CD₃OD/CDCl₃) δ (ppm) = 8.03 (s, 1H), 7.50 (s, 1H), 7.03 (s, 1H), 3.96 (s, 1H), 3.54 (s, 1H); ¹³C NMR (100 MHz, CD₃OD/CDCl₃) δ (ppm) = 161.58, 154.57, 147.46, 145.70, 143.49, 115.54, 109.09, 107.10, 55.93, 33.87. MS (ES⁺): 207.4 (M + H)⁺.

7-Methoxy-3-methyl-6-(2-quinolin-2-ylethoxy)quinazolin-4(3H)-one (27). 6-Hydroxy-7-methoxy-3-methylquinazolin-4(3H)-one was converted to the title compound in 67% yield (65 mg) using the coupling conditions as detailed for compound 16. ¹H NMR (400 MHz, CDCl₃) δ (ppm) = 8.07 (d, *J* = 8.5 Hz, 1H), 8.04 (d, *J* = 8.4 Hz, 1H), 7.91 (s, 1H), 7.76 (d, *J* = 7.8 Hz, 1H), 7.69 (s, 1H), 7.65 (m, 1H), 7.47 (m, 1H), 7.41 (d, *J* = 8.4 Hz, 1H), 7.05 (s, 1H), 4.63 (t, *J* = 6.9 Hz, 2H), 3.92 (s, 3H), 3.56–3.53 (m, 5H); ¹³C NMR (100 MHz, CDCl₃) δ (ppm) = 161.12, 158.87, 155.36, 148.89, 148.22, 145.75, 144.79, 136.52, 129.67, 129.23, 127.70, 127.18, 126.21, 122.20, 115.59, 108.18, 107.20, 68.59, 56.41, 38.64, 34.26; MS (ES⁺): 362.5 (M + H)⁺.

Biology Experimental Data. *PDE10 Enzyme Assay Protocol.* PDE10A was generated from the full-length recombinant rat clone transfected into Sf9 cells. The enzyme was extracted from cell pellets in lysis buffer (20 mM Tris, 2 mM benzamidine, 1.0 mM Na₂EDTA, 0.25 M sucrose, 100 μ M PMSF, pH 7.5 at room temperature) and stored frozen at –80 °C. PDE activity was measured using a plate based Scintillation Proximity Assay (SPA) modified from an Amersham Biosciences protocol (TRKQ7090). The K_m of the PDE10A preparation was experimentally determined to be 24 nM at room temperature. For competitive enzyme inhibition assays, the substrate [³H]cAMP concentration (New England Nuclear NET27500) was held at 20 nM for conditions to be at or below the K_m of the enzyme. The concentration of enzyme was adjusted to convert less than 10% of available substrate to end product during the assay. Compounds were initially dissolved in DMSO and diluted such that the final DMSO assay concentration was 3%. Following the addition of the test agents and [³H] cAMP, enzyme was added in buffer containing 50 mM Tris and 1.3 mM MgCl₂ (pH 7.5) to a final volume of 50 μ l. The incubation was allowed to proceed for 30 min at room temperature before the addition of 20 μ l of PDE SPA beads (Amersham Biosciences; RPNQ0150) at 0.2 mg/well to stop the reaction. Plates were allowed to stand 10 to 12 h before counting in a Trilux plate reader. IC₅₀s were calculated after the subtraction of background as determined by addition of 10 μ M papaverine.

■ ASSOCIATED CONTENT

S Supporting Information. PDE selectivity data for 16, 24, 26, and 27, X-ray crystal structure experimental data, PDE10A assay data with standard error, effects of compounds 25, 26, and 27 on striatal cGMP levels, and effect of compound 26 on conditioned avoidance responding (CAR) in wild type and PDE10A knockout mice. This material is available free of charge via the Internet at <http://pubs.acs.org>.

Accession Codes

Information has been deposited with Protein Databank as the following codes: 1, 2O8H; 2, 3HQW; 13, 3QPO; 16, 3QPP; 24, 3QPN.

■ AUTHOR INFORMATION

Corresponding Author

*Tel: (860) 715-5064. Fax: (860) 686-5291. E-mail: chris.j.helal@pfizer.com. Address: MS 8220-4326, Eastern Point Road, Groton, CT 06340.

■ ABBREVIATIONS USED

(±), indicates a racemic compound; Gln, glutamine; ADME, Absorption, Distribution, Metabolism, Excretion; CAR, conditioned avoidance responding; cAMP, cyclic adenosine monophosphate; cGMP, cyclic guanosine monophosphate; HBA, hydrogen bond acceptor; HLM Cl_{int}, human liver microsomal intrinsic clearance; HPLC, high performance liquid chromatography; MDR BA/AB, ratio of Basil to Apical/Apical to Basal permeability in a canine kidney cell line overexpressing the human multidrug resistant transporter (aka P-glycoprotein) with flux measured as 10^{–6} cm/sec; MW, molecular weight; PDE, phosphodiesterase; Pgp, p-glycoprotein; Phe, phenylalanine; STHIQ, sulfonyl tetrahydroisoquinoline; TPSA, topological polar surface area; Tyr, tyrosine; Val, valine

■ REFERENCES

- (1) Jeon, Y. H.; Heo, Y. S.; Kim, C. M.; Hyun, Y. L.; Lee, T. G.; Ro, S.; Cho, J. M. Phosphodiesterase: Overview of Protein Structures, Potential Therapeutic Applications and Recent Progress in Drug Development. *Cell. Mol. Life Sci.* **2005**, *62*, 1198–1220.
- (2) (a) Manallack, D. T.; Hughes, R. A.; Thompson, P. E. The Next Generation of Phosphodiesterase Inhibitors: Structural Clues to Ligand and Substrate Selectivity of Phosphodiesterases. *J. Med. Chem.* **2005**, *48*, 3449–3462. (b) Card, G. L.; England, B. P.; Suzuki, Y.; Fong, D.; Powell, B.; Lee, B.; Luu, C.; Tabrizizad, M.; Gillette, S.; Ibrahim, P. N.; Artis, D. R.; Bollag, G.; Milburn, M. V.; Kim, S.-H.; Schlessinger, J.; Zhang, K. Y. J. Structural Basis for the Activity of Drugs That Inhibit Phosphodiesterases. *Structure (Cambridge, MA, U. S. A.)* **2004**, *12*, 2233–2247.
- (3) (a) Chappie, T. A.; Humphrey, J. M.; Allen, M. P.; Estep, K. G.; Fox, C. B.; Lebel, L. A.; Liras, S.; Marr, E. S.; Menniti, F. S.; Pandit, J.; Schmidt, C. J.; Tu, M.; Williams, R. D.; Yang, F. V. Discovery of a Series of 6,7-Dimethoxy-4-pyrrolidylquinazoline PDE10A Inhibitors. *J. Med. Chem.* **2007**, *50*, 182–185. (b) Verhoest, P. R.; Chapin, D. S.; Corman, M.; Fonseca, K.; Harms, J. F.; Hou, X.; Marr, E. S.; Menniti, F. S.; Nelson, F.; O'Connor, R.; Pandit, J.; Proulx-LaFrance, C.; Schmidt, A. W.; Schmidt, C. J.; Suiciak, J. A.; Liras, S. Discovery of a Novel Class of Phosphodiesterase 10A Inhibitors and Identification of Clinical Candidate 2-[4-(1-Methyl-4-pyridin-4-yl-1H-pyrazol-3-yl)-phenoxy-methyl]-quinoline (PF-2545920)(I) for the Treatment of Schizophrenia. *J. Med. Chem.* **2009**, *52*, 5188–5196. (c) Hoefgen, N.; Stange, H.; Schindler, R.; Lankau, H.-J.; Grunwald, C.; Langen, B.; Egerland, U.; Tremmel, P.; Pangalos, M. N.; Marquis, K. L.; Hage, T.; Harrison, B. L.; Malamas, M. S.; Brandon, N. J.; Kronbach, T. Discovery of Imidazo[1,5-*a*]pyrido[3,2-*e*]pyrazines as a New Class of Phosphodiesterase 10A Inhibitors. *J. Med. Chem.* **2010**, *53*, 4399–4411.
- (4) (a) Seeger, T. F.; Bartlett, B.; Coskran, T. M.; Culp, J. S.; James, L. C.; Krull, D. L.; Lanfear, J.; Ryan, A. M.; Schmidt, C. J.; Strick, C. A.; Varghese, A. H.; Williams, R. D.; Wylie, P. G.; Menniti, F. S. Immunohistochemical Localization of PDE10A in the Rat Brain. *Brain Res.* **2003**, *985*, 113–126. (b) Schmidt, C. J.; Chapin, D. S.; Cianfrogna, J.; Corman, M. L.; Hajos, M.; Harms, J. F.; Hoffman, W. E.; Lebel, L. A.; McCarthy, S. A.; Nelson, F. R.; Proulx-LaFrance, C.; Majchrzak, M. J.; Ramirez, A. D.; Schmidt, K.; Seymour, P. A.; Suiciak, J. A.; Tingley, F. D., III; Williams, R. D.; Verhoest, P. R.; Menniti, F. S. Preclinical Characterization of Selective Phosphodiesterase 10A Inhibitors: A New Therapeutic Approach to the Treatment of Schizophrenia. *J. Pharmacol. Exp. Ther.* **2008**, *325*, 681–690.
- (5) (a) Suiciak, J. A.; Chapin, D. S.; Harms, J. F.; Lebel, L. A.; McCarthy, S. A.; Chambers, L.; Shrikhande, A.; Wong, S.; Menniti, F. S.; Schmidt, C. J. Inhibition of the Striatum-Enriched Phosphodiesterase PDE10A: A Novel Approach to the Treatment of Psychosis. *Neuropharmacology* **2006**, *51*, 386–396. (b) Strick, C. A.; Schmidt, C. J.; Menniti, F. S. PDE10A: A Striatum-Enriched, Dual-Substrate Phosphodiesterase. *Cyclic Nucleotide Phosphodiesterases Health Dis.* **2007**, 237–254.
- (6) Feng, B.; Mills, J. B.; Davidson, R. E.; Mireles, R. J.; Janiszewski, J. S.; Troutman, M. D.; de Morais, S. M. In vitro P-glycoprotein Assays to

Predict the In Vivo Interactions of P-Glycoprotein with Drugs in the Central Nervous System. *Drug Metab. Dispos.* **2008**, *36*, 268–275.

(7) (a) Sugiyama, A.; Satoh, Y.; Hashimoto, K. Electropharmacologic Effects of A New Phosphodiesterase III Inhibitor, Toborinone (OPC-18790), Assessed in An In Vivo Canine Model. *J. Cardiovasc. Pharmacol.* **2001**, *38*, 268–277. (b) Van de Water, A.; D'Aubioul, J.; Van Gerven, W.; De Chaffoy de Courcelles, D.; Freyne, E.; Xhonneux, R.; Reneman, R. S.; Janssen, P. A. J. Cardiac and Hemodynamic Effects of Intravenous R 80122, A New Phosphodiesterase III Inhibitor, In Anesthetized and Awake Dogs. *Arch. Int. Pharmacodyn. Ther.* **1992**, *316*, 60–74.

(8) Pandit, J. Crystal Structure of 3',5'-Cyclicnucleotide Phosphodiesterase (PDE10A) and Uses Thereof. U.S. Pat. Appl. Publ. 0202550, 2005.

(9) (a) Gleeson, M. P. Generation of a Set of Simple, Interpretable ADMET Rules of Thumb. *J. Med. Chem.* **2008**, *51*, 817–834. (b) Clark, D. E. Rapid Calculation of Polar Molecular Surface Area and Its Application to the Prediction of Transport Phenomena. 2. Prediction of Blood-Brain Barrier Penetration. *J. Pharm. Sci.* **1999**, *88*, 815–821. (c) Doan, K. M. M.; Humphreys, J. E.; Webster, L. O.; Wring, S. A.; Shampine, L. J.; Serabjit-Singh, C. J.; Adkison, K. K.; Polli, J. W. Passive Permeability and P-Glycoprotein-Mediated Efflux Differentiate Central Nervous System (CNS) and Non-CNS Marketed Drugs. *J. Pharmacol. Exp. Ther.* **2002**, *303*, 1029–1037.

(10) Separation of enantiomers in a structurally related analog (*p*-methoxy phenyl) resulted in one enantiomer demonstrating significantly more PDE10 and PDE3A/B activity (>20×) than the other. As such, the use of the racemic 3-phenylpiperidine was deemed feasible for assessing selectivity.

(11) Gehlhaar, D. K.; Verkhivker, G. M.; Rejto, P. A.; Sherman, C. J.; Fogel, D. B.; Fogel, L. J.; Freer, S. T. Molecular Recognition of the Inhibitor AG-1343 by HIV-1 Protease: Conformationally Flexible Docking by Evolutionary Programming. *Chem. Biol.* **1995**, *2*, 317–324.

(12) Marrone, T. J.; Luty, B. A.; Rose, P. W. Discovering High-Affinity Ligands from the Computationally Predicted Structures and Affinities of Small Molecules Bound to A Target: A Virtual Screening Approach. *Perspect. Drug Discovery Des.* **2000**, *20*, 209–230.

(13) If all reagents were mixed together at the same time, products from the addition of 5 to the azodicarboxylate were observed with little product. See: Hughes, D. L. The Mitsunobu Reaction. *Org. React. (Hoboken, NJ, U. S. A.)* **1992**, *42*.

(14) Helal, C. J. Heteroaromatic Quinoline Compounds as Phosphodiesterase Inhibitors, Their Preparation, Pharmaceutical Compositions, and Use in Treating CNS and Other Disorders. WO 2008/020302 A2, 2008.

(15) Hopkins, A. L.; Groom, C. R.; Alex, A. Ligand Efficiency: A Useful Metric for Lead Selection. *Drug Discovery Today* **2004**, *9*, 430–431.

(16) Lombardino, J. G. Pharmaceutical Imidazoles. Ger. Offen. DE 2155558, 1972.